BIOCHEMICAL AND MOLECULAR TOXICOLOGY **WILEY**

Biologically active phthalocyanine metal complexes: Preparation, evaluation of α-glycosidase and anticholinesterase enzyme inhibition activities, and molecular docking studies

Emre Güzel[1] | Ümit M. Koçyiğit[2] | Parham Taslimi[3] | Sultan Erkan[4] | Omer S. Taskin[5]

[1]Department of Fundamental Sciences, Sakarya University of Applied Sciences, Sakarya, Turkey

[2]Department of Basic Pharmaceutical Sciences, Sivas Cumhuriyet University, Sivas, Turkey

[3]Department of Biotechnology, Bartın University, Bartın, Turkey

[4]Department of Chemistry, Sivas Cumhuriyet University, Sivas, Turkey

[5]Department of Chemical Oceanography, İstanbul University, İstanbul, Turkey

Correspondence
Emre Güzel, Department of Fundamental Sciences, Sakarya University of Applied Science, Sakarya 54050, Turkey.
Email: eguzel@subu.edu.tr

Ümit M. Koçyiğit, Department of Basic Pharmaceutical Sciences, Cumhuriyet University, Sivas 58140, Turkey.
Email: ukocyigit@cumhuriyet.edu.tr

Abstract

In this study, preparation, as well as investigation of α-glycosidase and cholinesterase (ChE) enzyme inhibition activities of furan-2-ylmethoxy-substituted compounds **1–7**, are reported. Peripherally, tetra-substituted copper and manganese phthalocyanines (**5** and **6**) were synthesized for the first time. The substitution of furan-2-ylmethoxy groups provides remarkable solubility to the complex and redshift of the phthalocyanines Q-band. Besides, the inhibitory effects of these compounds on acetylcholinesterase (AChE), butyrylcholinesterase (BChE), and α-glycosidase (α-Gly) enzymes have been investigated. The AChE was inhibited by these compounds (**1–7**) in low micromolar levels, and K_i values were recorded between 11.17 ± 1.03 and $83.28 \pm 11.08\,\mu M$. Against the BChE, the compounds demonstrated K_i values from 7.55 ± 0.98 to $81.35 \pm 12.80\,\mu M$. Also, these compounds (**1–7**) effectively inhibited α-glycosidase, with K_i values in the range of 744.87 ± 67.33 to $1094.38 \pm 88.91\,\mu M$. For α-glycosidase, the most effective K_i values of phthalocyanines **3** and **6** were with K_i values of 744.87 ± 67.33 and $880.36 \pm 56.77\,\mu M$, respectively. Moreover, the studied metal complexes were docked with target proteins PDB ID: 4PQE, 1P0I, and 3WY1. Pharmacokinetic parameters and secondary chemical interactions that play an active role in interaction were predicted with docking simulation results. Overall, furan-2-ylmethoxy-substituted phthalocyanines can be considered as potential agents for the treatment of Alzheimer's diseases and diabetes mellitus.

KEYWORDS
cholinesterases, enzyme inhibition, molecular docking, phthalocyanine, α-glycosidase

1 | INTRODUCTION

Although the origin of porphyrin chemistry dates back to Hans Fischer in the 1930s, the synthesis of these macrocyclic compounds and the preparation of new macrocyclic species continuously is a matter of scientific interest. Phthalocyanines (Pcs), besides being one of the most studied macrocyclic compounds, are the best-known synthetic porphyrin analogs. These macrocycles are widely studied compounds for many high-tech applications, such as photovoltaic cells,[1,2] chemical sensors,[3] electrochromic materials,[4] Langmuir Blodgett films,[5] liquid crystals,[6] and

photodynamic cancer therapy.[7,8] Among these applications, the use of phthalocyanines as an enzyme inhibitor has attracted attention in recent years.[9,10] Providing the solubility of phthalocyanines is very important for use in these application areas.[11] The solubility of phthalocyanine complexes, especially evaluated for biological applications, such as anticancer and enzyme inhibition, is very important for increasing the effectiveness of the compounds. The introduction of various substituents in peripheral, nonperipheral, or axial positions and extension of π-electron density have a strong effect on the electronic and absorption properties as well as increasing the solubility properties of Pcs.[12–15]

α-Glycosidase is an enzyme of the glycoside family of hydrolases that hydrolyzes the α-glycosidic bonds in carbohydrate molecules. The inhibition of α-glucosidase is very important for the design of antidiabetic drugs because it prevents the postprandial increase in blood sugar levels in diabetic patients by reducing the digestion of carbohydrates. Inhibition of α-glycosidase helps to slowly release monosaccharide molecules into the bloodstream after a meal.[16,17] In 1940, Allis and Hawes discovered two major forms of cholinesterase (ChE) enzymes, acetylcholinesterase (AChE) and butyrylcholinesterase (BChE). These two enzymes are present in the human body. The AChE enzyme is found in neuromuscular connections in muscle tissue, red blood cell cells, and cholinergic nerve synapses, whereas BChE is present in the liver, plasma, nervous system, and pancreas. BChE and AChE belong to the class of serine hydrolases.[18,19] The difference in amino acid residues from the active sites BChE and AChE determines the different properties of the substrates and inhibitors of these enzymes. These are important components of the brain's cholinergic synapses and neuromuscular connections. The main function of BChE and AChE is the catalytic hydrolysis of the neurotransmitter acetylcholine and the termination of nerve impulses in cholinergic synapses.[20]

In this study, to investigate some metabolic enzyme inhibition properties, the furan-2-ylmethoxy group containing phthalonitrile derivative and its phthalocyanine complexes have been obtained. The studied compounds showed good solubility and were also recorded as anticholinergic and antidiabetic potentials.

2 | MATERIALS AND METHODS

2.1 | Instruments and chemicals

UV–Vis studies were carried out by a Shimadzu UV-1280 spectrophotometer. Infrared and NMR spectra were performed on a Perkin-Elmer Fourier transform infrared (FT-IR) spectrophotometer and a Bruker 300 MHz spectrometer, respectively. The MALDI Synapt G2-Si Mass Spectrometry was used to take Mass spectra (MS). 2,5-dihydroxybenzoic acid was used as the matrix for MALDI-TOF mass spectrometry. All solvents and starting materials were purchased from Merck Chemical Company. 4-(furan-2-ylmethoxy) phthalonitrile (**1**) and its soluble zinc, indium, gallium, and metal-free phthalocyanine derivatives (**2**, **3**, **4**, and **7**) were prepared according to the reported procedures.[21,22]

2.1.1 | General procedure for the synthesis of the phthalocyanine complexes (5, 6)

The phthalonitrile derivative (**1**) (0.100 g, 0.36 mmol), anhydrous $CuCl_2$ and $MnCl_2$ ~(0.030 g) in the presence of amyl alcohol and 1,8-diazabicyclo-[5.4.0]-7-undecene (DBU; 0.05 ml) were heated in a sealed tube under an argon atmosphere for 10 h. After completion of the reaction, the resulting green mixture was cooled to room temperature. The crude products were precipitated by diethyl ether and then washed with ethyl acetate. The crude products were further purified by column chromatography using a mixture of CH_2Cl_2:EtOH (10:1 v/v) as an eluent. The obtained Pcs **5** and **6** were highly soluble in ethyl acetate, dimethylsulfoxide, dimethylformamide, CH_2Cl_2, and $CHCl_3$.

Yield of **5**: 42 mg (39.8%). M.p. > 200°C. FT-IR (v_{max} cm^{-1}): 3,012 (m, Ar. C–H), 2,950 (–CH_3), 1,622 (m, Ar. –C=C), 1,477 (m, Aliph. C-H), and 1,122 (s, –C–O–C). UV-vis λ_{max} (nm) tetrahydrofuran (THF): 680 and 348. Anal. Calc. For $C_{52}H_{32}CuN_8O_8$: C, 65.03; H, 3.36; Cu, 6.62; N, 11.67; O, 13.33; Found: C, 65.66; H, 3.25; N, 12.76. MS (MALDI-TOF): m/z 977.10 [M+H_2O]$^+$.

Yield of **6**: 48 mg (45.4%). M.p. > 200°C. FT-IR (v_{max} cm^{-1}): 3,022 (m, Ar. C–H), 2,962 (–CH_3), 1,678 (m, Ar. –C=C), 1,488 (m, Aliph. C–H), and 1,166 (s, –C–O–C). UV-vis λ_{max} (nm) THF: 730, 503, and 365. Anal. Calc. For $C_{52}H_{32}MnN_8O$: C, 65.62; H, 3.39; Mn, 5.77; N, 11.77; O, 13.45; Found: C, 65.52; H, 3.23; N, 11.96. MS (MALDI-TOF): m/z 970.08 [M+ H_2O]$^+$.

2.2 | Enzyme studies

The inhibitory efficacy of compounds **1–7** on BChE/AChE activities was obtained conforming to the spectrophotometric procedure of Ellman et al.[23] and also performed according to our previous study.[24–27] Besides, the inhibitory effect of these compounds on α-Gly enzyme activity was carried out using the p-nitrophenyl-D-glycopyranoside (p-NPG) substrate according to the analysis of Tao et al.[28] Those graphs obtained the IC$_{50}$ values. Three different novel concentrations of phthalocyanine complexes were used to calculate K_i values. In this study, graphs were given which are exhibited for the most effective inhibition of the studied compounds. According to this method, measurements were made every 5 min at a wavelength of 412 nm. Related graphs were created for the inhibition values of each molecule (%).

2.3 | Molecular docking studies

Molecular docking studies allow examining the biological activity of molecules at the molecular level. This virtual scanning technique pre-

dicts binding energies, binding poses, and intermolecular interactions between the developed compounds and biological systems with high accuracy.[29] In this way, molecular docking studies provide useful information in drug designs. The PDB ID: 4PQE, 1P0I[30], and 3WY1[31] target proteins representing the crystal structure of acetylcholinesterase (AChE), butyrylcholinesterase (BChE), and α-glycosidase (α-Gly) enzymes, respectively, were obtained from the protein data bank. Since metallophthalocyanine complexes are multiatom molecules, the complexes geometry was drawn and optimized with the Docking Server system. Geometry optimization of metallophthalocyanine complexes was performed by the MMFF94 method. The charge calculation method was chosen as Gasteiger. In all calculations, pH7.0 was preferred. In docking calculations, grid maps were selected as 90 × 90 × 90 Å (x, y, and z) and Lamarckian genetic algorithm and Solis & Wets local search method were used.[32] During docking, the population size was set to 150. A translation step of 0.2 Å, as well as quaternion and torsion steps of 5 Å, were applied during the search for the appropriate region of the target protein of the molecules studied.

3 | RESULTS AND DISCUSSION

3.1 | Synthesis and characterization

Figure 1 represents the synthetic route of novel soluble metal-free and metallophthalocyanine complexes 2–7.

Targeted peripherally substituted phthalocyanines 5 and 6 were prepared by using the metal salts in 1,8-diazabicyclo-[5.4.0]-7-undecene (DBU). The reactions were carried out by using DBU and metal salts (CuCl$_2$ for 5 and Mn(CH$_3$COO)$_2$ for 6) and appropriate solvents (amyl alcohol) at 145°C. The crude complexes were isolated after washing with ethyl acetate. The yields obtained for the copper and manganese phthalocyanines 5 and 6 are 40% and 45%, respectively. Elucidation of the newly phthalocyanine complexes was performed with ultraviolet-visible spectrophotometry, elemental analysis, ^{1}H-NMR (nuclear magnetic resonance) spectroscopy, FT-IR, and MALDI-TOF mass spectrometry. In the FT-IR spectrum of phthalocyanines, the peak of the C≡N vibration of compound 1 at 2,227 cm^{-1} disappeared as expected. Stretching vibrations of aliphatic C–H bonds of phthalocyanines, as in the phthalonitrile derivative, were detected at around 2,955 cm^{-1}. Similarly, stretching vibrations of aromatic C–H bonds of phthalocyanines 2–6 were observed at around 3015 cm^{-1}. ^{1}H-NMR investigations of complexes 2, 3, 4, and 7 provided the expected chemical changes for the structure.[22] Due to the paramagnetic character of copper, manganese, and cobalt, there is no signal for the phthalocyanines 4, 5, and 6 in ^{1}H-NMR spectroscopy. Besides, it has been found that the complexes synthesized in the structures observed without significant fragmentation are stable under MALDI-MS conditions. The molecular ion peaks were observed at m/z: 977.10 [M+H$_2$O]$^+$ for 5 and 970.08 [M+H$_2$O]$^+$ for 6.

3.2 | UV-Vis absorption studies

The first and most common method used to understand whether phthalocyanine complexes are formed is absorption spectroscopy. These complexes show typical electronic spectra with two absorption regions. One of them in the UV region at about 300–350 nm (B band) and the other one in the visible area at 600–700 nm (Q-band). UV-vis absorption spectra of the MPcs are compared in the
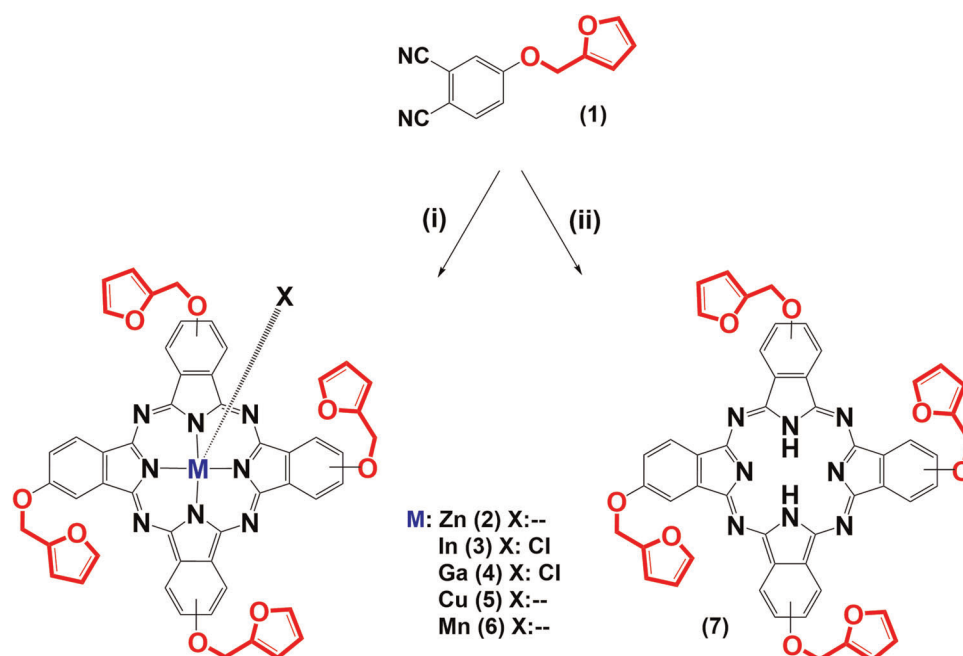

FIGURE 1 The synthetic scheme of soluble metal-free and metallophthalocyanines 2–7 (i) 1,8-diazabicyclo-[5.4.0]-7-undecene (DBU), amyl alcohol, metal salts, 145°C (ii) DBU, dimethylformamide, 145°C
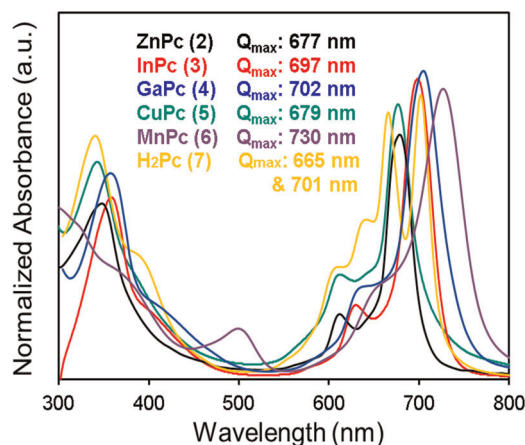
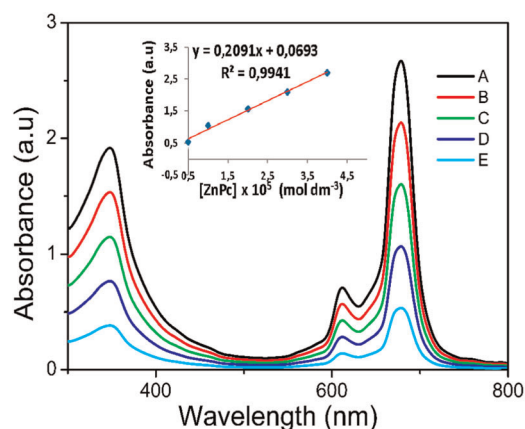**FIGURE 2** Normalized absorption spectra of the soluble peripherally substituted phthalocyanines **2–7** in THF

FIGURE 3 Electronic absorption spectra of zinc phthalocyanine **2** (ZnPc) in THF at different concentrations: (A) 40×10^{-6}, (B) 30×10^{-6}, (C) 20×10^{-6}, (D) 10×10^{-6}, (E) 5×10^{-6} mol dm^{-3}. The inset shows calibration plot for Q-band maximum

THF solution. As can be seen, the absorption spectra in the THF solution exhibit a typical phthalocyanine Q band around 650–700 nm accompanied by a weak vibronic band around 615–630 nm.[8,33] The solution spectra show a spectral characteristic, indicating D$_{4h}$ symmetry, which is typical for phthalocyanine complexes.[34] The absorption peak in the near-UV region is the B-band or Soret band that is attributed to the $a_{2u} \rightarrow e_g^*$ transition; a further band in the visible region is related to the Q-band caused by the π–π* transition $a1u \rightarrow e_g^*$. It can be stated that there are some vibrational bands at relatively shorter wavelengths, which are a standard property of metallophthalocyanine.[35] In the UV–vis spectra of the obtained phthalocyanines, the Q bands, which are one of the characteristic bands for phthalocyanines and observed in the visible part, were seen at 677 nm for **2**, 697 nm for **3**, 702 nm for **4**, 679 nm for **5**, 730 nm for **6**, and 665, 701 nm for **7** (Figure 2).

In metallophthalocyanine complexes **2–7**, the single (narrow) Q bands showed that these phthalocyanines are in monomeric form in the solvent medium. All complexes demonstrated intense single Q-absorption bands, which are indicative of the metallophthalocyanines with the D$_{4h}$ symmetry.[34,36] Also, indium, gallium, and manganese phthalocyanine complexes **3**, **4**, and **6** showed redshift when compared to other metallophthalocyanine complexes in this study. This situation could be interpreted by the fact that the larger gallium, indium, and manganese atoms are located out of the plane of the phthalocyanine cavity for complexes **3**, **4**, and **6**. Aggregation can be explained as a very tight stacking of monomers, dimers, and rings in the studied solvent. There are many parameters in phthalocyanines that affect aggregation, such as concentration, peripheral and nonperipheral substituents, nature of the solvent, operating temperature, and the metal ion in the macrocyclic nucleus.

To better observe the solubility and aggregation properties of the phthalocyanines, dilution studies were performed in THF solvent. As an illustrative example, peripherally substituted zinc

TABLE 1 The enzyme inhibition results of phthalocyanines (**1–7**) against butyrylcholinesterase (BChE), acetylcholinesterase (AChE), and α-glycosidase (α-Gly) enzymes

| Compounds | IC$_{50}$ (μM) | | | | | | K$_i$ (μM) | | |
	AChE	r^2	BChE	r^2	α-Gly	r^2	AChE	BChE	α-Gly
1	38.35	.9738	17.47	.9373	983.27	.9205	30.24 ± 6.43	13.84 ± 2.14	1,032.14 ± 83.24
2	104.37	.9722	83.20	.9889	902.83	.9783	83.28 ± 11.08	67.61 ± 9.43	945.25 ± 56.22
3	81.04	.9488	103.22	.9904	804.34	.9584	67.83 ± 16.51	81.35 ± 12.80	880.36 ± 56.77
4	19.26	.9705	24.05	.9912	1,034.89	.9823	14.66 ± 2.07	21.46 ± 2.55	1,094.38 ± 88.91
5	15.91	.9673	11.27	.9688	911.20	.9542	11.17 ± 1.03	7.55 ± 0.98	957.21 ± 93.08
6	48.04	.9814	59.37	.9082	695.37	.9346	38.98 ± 5.82	47.42 ± 5.98	744.87 ± 67.33
7	94.37	.9572	76.22	.9824	1,104.04	.9898	69.08 ± 13.77	59.03 ± 9.01	1,073.11 ± 103.24
TAC[a]	145.31	.9734	208.03	.9881	-	-	112.05 ± 24.05	177.15 ± 39.05	-
ACR[b]	-	-	-	-	0.38	.9703	-	-	0.57 ± 0.11

[a]Tacrine (TAC) was used as a control for AChE and BChE enzymes.

[b]Acarbose (ACR) was used as a control for the α-glycosidase enzyme.

phthalocyanine complex **2** was carried out using concentrations ranging from 5 to 40 μM (Figure 3).

3.3 | Enzyme results

3.3.1 | AChE and BChE inhibition results

ChE enzyme inhibitors are extensively used in medicine for the pharmacological correction of cholinergic neurotransmission pathologies. The efficacy of anti-ChEs drugs is based on their capability to potentiate the effects of ACh molecule by reducing the rate of ChEs-catalyzed hydrolysis of ACh molecule. Indeed, an extension of the lifetime of ACh molecules can compensate cholinergic abnormalities in disturbances of neuromuscular synaptic transmission and Alzheimer's disease (AD). All the compounds (**1–7**) had significantly higher AChE inhibitory activity than that of standard AChE inhibitors, such as Tacrine (TAC). Furthermore, the K_i values of the phthalonitrile derivative and its complexes (**1–7**) and standard compound (TAC) are summarized in Table 1. As can be seen from the results obtained in Table 1 and Figure 4, these compounds (**1–7**) effectively inhibited AChE, with K_i values in the range of 11.17 ± 1.03 to 83.28 ± 11.08 μM. However, all the compounds (**1–7**) had almost similar inhibition profiles. The most active **5** showed K_i values of 11.17 ± 1.03 nM. For AChE, IC_{50} values of TAC as positive control and some novel compounds were studied in this study in the following order: **5** (15.91 μM, r^2:.9673) < **4** (19.26 μM, r^2:.9705) < **1** (38.35 μM, r^2:.9738) < **6** (48.04 μM, r^2:.9814) < **TAC** (145.31 μM, r^2:.9734). For BChE, IC_{50} values of TAC as positive control and novel phthalocyanine complexes **1–7** in the following order: **5** (11.27 μM, r^2:.9688) < **1** (17.47 μM, r^2:.9373) < **4** (24.05 μM, r^2:.9912) < **6** (59.37 μM, r^2:.9082) < **TAC** (208.03 μM, r^2:.9881). Additionally, the novel compounds effectively inhibited BChE, with K_i values in the range of 7.55 ± 0.98 to 81.35 ± 12.80 μM. However, all of these compounds (**1–7**) had almost similar inhibition profiles. The most active compound **5** and **1** effectively inhibited BChE, with K_i values of 7.55 ± 0.98 to 13.84 ± 2.14 μM.

3.3.2 | α-Glycosidase inhibition results

Many organisms naturally produce inhibitors of α-glycosidase, and various inhibitors have been recorded to date; some are being already utilized for the treatment aim. Many microorganisms and plants have been recorded to produce glycosidase inhibitors, but those which produce molecules that mimic the structure of oligosaccharide or monosaccharide are very efficient because they resemble the sugar moiety of natural substrate. For enzyme glycosidase, phthalocyanines **1–7** have IC_{50} values in the range of 0.82–1.94 nM and Ki in the range of 1.56 ± 0.32-14.78 ± 2.57 μM (Table 1 and Figure 4). The results have documented that all of these phthalocyanines (**1–7**) have shown the inhibitory effects of
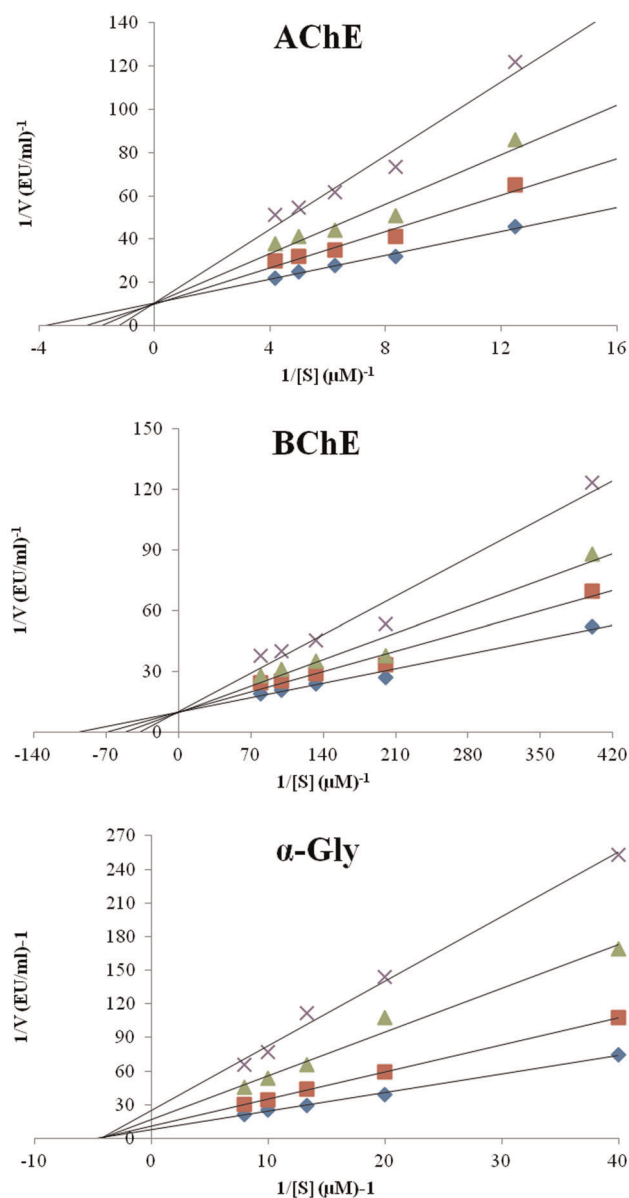

FIGURE 4 Determination of Lineweaver–Burk graphs for excellent inhibitors of acetylcholinesterase (AChE) for phthalocyanine **5**, butyrylcholinesterase (BChE) for phthalocyanine **5**, and α-glycosidase (α-Gly) for phthalocyanine **6**, respectively

α-glycosidase efficient acarbose (IC_{50}: 0.38 μM) as a standard glycosidase inhibitor. The most effective K_i values of phthalocyanine complexes **6** and **3** were with K_i values of 1.56 ± 0.32 and 2.68 ± 0.65 μM, respectively. For α-glycosidase, IC_{50} values of ACR as positive control and compounds (**1–7**) are in the following order: **ACR** (0.38 μM, r^2:.9703) < **6** (0.82 μM, r^2:.9724) < **3** (1.94 μM, r^2:.9728) < **2** (2.94 μM, r^2:.9835). In general, such compounds give results on these metabolic enzymes at the micromolar level. Therefore, these compounds are very crucial for drug production. As is known, some α-glucosidase inhibitors exhibit efficient antidiabetic properties. Indeed, the most effective way to improve glucose control in patients with type 2 diabetes mellitus (T2DM) consists of a proper

TABLE 2 The docking energy results between the investigated phthalocyanines with the related target proteins

Compound	4PQE (AChE)		1P0I (BChE)		3WY1 (α-Gly)	
	Est. free energy of binding	vdW + Hbond + desolv energy	Est. free energy of binding	vdW + Hbond + desolv energy	Est. free energy of binding	vdW + Hbond + desolv energy
2	−7.06	−9.94	−4.08	−6.11	−6.67	−7.84
3	−6.54	−7.33	−4.05	−5.73	−7.64	−8.05
4	−5.85	−6.28	−5.03	−7.27	−5.52	−6.21
5	−7.23	−8.79	−5.21	−7.67	−6.50	−7.70
6	−6.87	−7.54	−4.23	−7.01	−7.99	−8.23
7	−6.44	−7.21	−4.14	−6.95	−7.46	−9.84

Abbreviations: AChE, acetylcholinesterase; BChE, butyrylcholinesterase; TAC, Tacrine; vdW, vdW + Hbond + desolv energy, van der Walls + H-bond + desolved energy; α-Gly, α-glycosidase.

diet of fat and carbohydrate, bodyweight reduction, physical activity, use of oral hypoglycemic agents, and insulin injection. T2DM treatments generally use oral hypoglycemic factors, as miglitol, acarbose, and voglibose. For instance, we preferred acarbose as standard in this study. Overall, these compounds can act in α-glycosidase inhibition activity, an enzyme located in the small intestine epithelium. Preventing the hydrolysis of carbohydrate molecules like glucose is an alternative to treatment and a therapeutic approach for T2DM.

3.4 | Molecular docking

Experimentally determined enzyme inhibition activity of some phthalocyanines was calculated with the help of simulation. Each phthalocyanine was individually docked into the determined target proteins as 4PQE, 1P0I, and 3WY1. The obtained estimated free binding energies and secondary chemical interaction energies (van der Walls + H-bond + desolved energy) are given in Table 2.

According to the docking results, the calculated AChE enzyme inhibition activity is very similar to the experimental sequence. The only difference in the docking results according to the experimental results between the 4PQE target protein and the phthalocyanines **2–7** is that the inhibition efficiency of the gallium phthalocyanine complex **4**, whose inhibition efficiency should be in the second place, has the lowest value. In other words, it is the calculation in the second row of the enzyme inhibition activity of the zinc phthalocyanine complex **2** with the experimentally lowest inhibition efficiency. This may be due to the high vdW + Hbond + desolv energy value of the zinc complex **2**. This complex with amino acid residues on target protein appears to be highly interacting, as given in Figure S6. The calculated estimated free binding energies for all other complexes are well in agreement with the experimental inhibition efficiency ranking. On the contrary, for the computational results of BcHE enzyme activity, all compounds were docked with the 1P0I target

protein. The estimated free binding energies of compounds **2–7** with the 1P0I target protein and vdW + Hbond + desolv energies showed a parallel trend, and these examined energy values are listed in Table 2. The binding poses and interaction modes between the studied phthalocyanines and the target protein representing the BcHE enzyme are given in Figure 5. Docking poses and interaction modes between **2–7** and other target proteins (PDB ID: 4PQE and 3WY1) were added to Figures S6 and S7, respectively. The order in the figures was made from the strongest to the lowest interaction between the drug candidate molecule and the target proteins.

As shown in Figure 5, copper phthalocyanine complex **5** with the highest inhibition efficiency formed an H-bond with the ASN245 amino acid residue of the 1P0I target protein. Also, this complex with the target protein interacts in polar, hydrophobic, and π–π interactions. ASN241 and ARG240 amino acid residues in polar interactions, TYR282, LEU249, PRO281, and LEU244 amino acid residues in hydrophobic interactions and TYR282 amino acid residues in π–π interactions play an active role in π–π interactions. If it examines the interaction modes of the gallium phthalocyanine complex **4** with the interested target protein, this complex exhibits H-bond, polar, hydrophobic, and π–π interactions as in the copper phthalocyanine complex **5**. However, amino acid residues playing an active role in interactions differ according to the type of interaction.[37,38] Complex **4** were formed the H-bond with the amino acid residue TYR282. The length of the H-bond between the nitrogen atom in the copper phthalocyanine complex **5** and ASN245 is 3.04 Å, whereas the length of the H-bond between the nitrogen atom in the gallium phthalocyanine complex **4** and the TYR282 amino acid residue is 3.35 Å. Therefore, the shorter H-bond length in the copper phthalocyanine complex **5** may have enhanced the interaction energy. Also, ARG282 and GLU 238 amino acid residues play a role in polar interaction; PRO281 and PRO359 amino acid residues in hydrophobic interaction; and TYR282 amino acid residue in π–π interaction in the gallium phthalocyanine complex **4**. There are polar, hydrophobic, and π–π interactions between the manganese phthalocyanine complex **6** and the 1P0I target protein. The

(5)-BChE
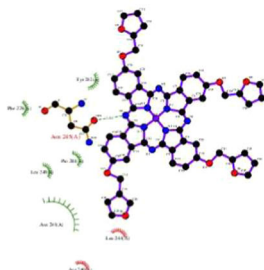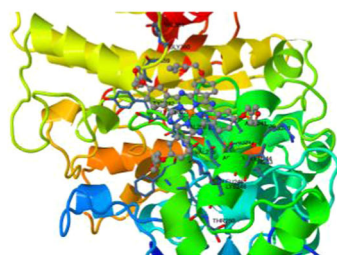
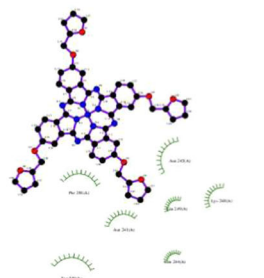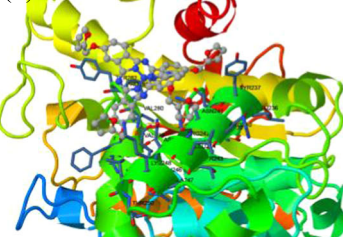| Hydrogen bonds	Polar	Hydrophobic	Pi-Pi
ASN245	ASN241	TYR282	TYR282
	ARG240	LEU249	
		PRO281	
		LEU244	

(4)-BChE
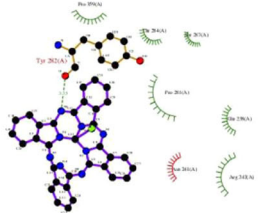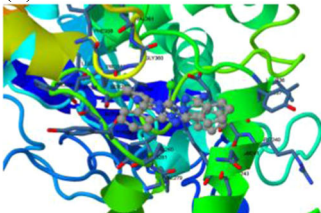
Hydrogen bonds	Polar	Hydrophobic	Pi-Pi
TYR282	ARG242	PRO281	TYR282
	GLU238	PRO359	

(6)-BChE

Polar	Hydrophobic	Pi-Pi
ASN245	TYR282	TYR237
ASN241	PRO281	
LYS248	LEU249	
	LEU244	

(7)-BChE
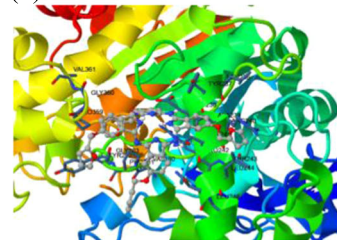
Hydrogen bonds	Polar	Cation-Pi	Hydrophobic	Pi-Pi
ASN241	ARG240	TYR237	PRO281	TYR232
			TYR282	TYR282
			LEU244	

(2)-BChE
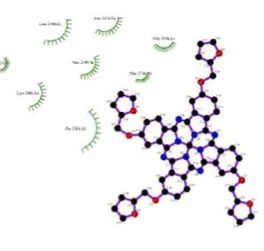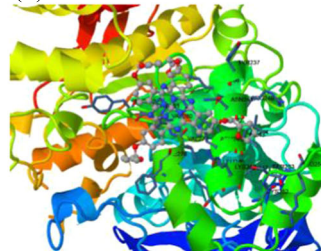
Polar	Hydrophobic	Pi-Pi
ASN241	PRO281	PHE278
ASN245	LEU244	
	PHE278	

(3)-BChE

Polar	Hydrophobic	Pi-Pi
ASN241	PRO281	PHE278
ASN245	PHE278	TYR282
	TYR282	

FIGURE 5 Docking poses and interaction modes between phthalocyanines **2–7** and 1P0I target protein

corresponding amino acid residues in these interactions are shown in Figure 5.

The phthalocyanine ligand, which is the main factor involved in the formation of complexes is formed a cation-π bond with amino acids, unlike complexes. Also, the excess in the number of interaction types of the metal-free phthalocyanine **7**, as shown in Figure 2, is thought to cause the high interaction energy given in Table 2. According to the order of inhibition efficiency, polar, hydrophobic, and π–π interactions in the zinc phthalocyanine complex **2** placed in Figure 5 draw attention. In these interactions, ASN241, ASN245, PRO281, and PHE278 amino acids are active. Finally, the ASN241, ASN245, PRO281, PHE278, and TYR282 amino acids are effective in polar, hydrophobic, and π–π interactions in the indium phthalocyanine complex **3**, which is placed in the appropriate position after docking.

4 | CONCLUSION

In conclusion, α-glycosidase, ChE enzyme inhibition activities of furan-2-ylmethoxy-substituted phthalocyanine derivatives are reported for the first time. The substitution of furan-2-ylmethoxy groups to the phthalocyanine ring not only increased the solubility of the complex but also ensured a significantly bathochromic shift of the Q-band. Experimental results were compared with standard molecules used in the relevant activities. The results obtained will certainly shed light on future biochemical, physiological, and pharmacological studies in the relevant fields, and the results will have important effects on the investigation and treatment of many metabolic diseases, such as Alzheimer's and diabetes. In this context, especially copper and manganese phthalocyanines are thought to make significant contributions to the design of drugs to be used for future treatment and related applications. Molecular docking studies were carried out for the effectiveness of AChE, BChE, and α-Gly enzyme inhibition of the synthesized phthalocyanines, and the calculated results were found to be quite compatible with the experimental data.

CONFLICT OF INTERESTS
The authors declare that there are no conflict of interests.

AUTHOR CONTRIBUTIONS
Designing the study: Emre Güzel and Ümit M. Koçyiğit. *Collecting and Analyzing the Data*: Parham Taslimi, Ümit M. Koçyiğit, and Omer S. Taskin. *Drafting the manuscript*: Emre Güzel. *Visualization and Revising*: Emre Güzel. *Theoretical calculations*: Sultan Erkan. *Supervision*: Emre Güzel, Ümit M. Koçyiğit.

DATA AVAILABILITY STATEMENT
The authors confirm that the data supporting the findings of this study are available within the article.

ORCID
Emre Güzel http://orcid.org/0000-0002-1142-3936
Ümit M. Koçyiğit https://orcid.org/0000-0001-8710-2912
Parham Taslimi http://orcid.org/0000-0002-3171-0633

Sultan Erkan https://orcid.org/0000-0001-6744-929X
Omer S. Taskin https://orcid.org/0000-0002-6284-1337

REFERENCES

[1] T. Keleş, Z. Biyiklioglu, E. Güzel, M. Nebioğlu, İ. Şişman, *Appl. Organomet. Chem.* **2021**, 35, e6076.

[2] B. Yıldız, E. Güzel, D. Akyüz, B. S. Arslan, A. Koca, M. K. Şener, *Sol. Energy* **2019**, 191, 654.

[3] T. V. Basova, N. S. Mikhaleva, A. K. Hassan, V. G. Kiselev, *Sens. Actuators, B* **2016**, 227, 634.

[4] E. Güzel, E. B. Orman, B. Köksoy, Ö. Çelikbıçak, M. Bulut, A. R. Özkaya, *J. Electrochem. Soc.* **2019**, 166, H438.

[5] R. J. G. Rubira, P. H. B. Aoki, C. J. L. Constantino, P. Alessio, *Appl. Surf. Sci.* **2017**, 416, 482.

[6] T. Basova, E. Kol'tsov, A. K. Ray, A. K. Hassan, A. G. Gürek, V. Ahsen, *Sens. Actuators, B* **2006**, 113, 127.

[7] L. Sobotta, J. Dlugaszewska, P. Kasprzycki, S. Lijewski, A. Teubert, J. Mielcarek, M. Gdaniec, T. Goslinski, P. Fita, E. Tykarska, *J. Photochem. Photobiol. B Biol.* **2018**, 183, 111.

[8] E. Güzel, A. Atsay, S. Nalbantoglu, N. Şaki, A. L. Dogan, A. Gül, M. B. Koçak, *Dyes Pigm.* **2013**, 97, 238.

[9] T. Arslan, Z. Biyiklioglu, M. Şentürk, *RSC Adv.* **2018**, 8, 10172.

[10] Ü. Demirbaş, B. Barut, A. Özel, H. Kantekin, *J. Mol. Struct.* **2019**, 1187, 8.

[11] B. Akkurt, E. Hamuryudan, *Dyes Pigm.* **2008**, 79, 153.

[12] E. Güzel, *RSC Adv.* **2019**, 9, 10854.

[13] Ö. Kurt, I. Özçeşmeci, A. Gül, M. B. Koçak, *J. Organomet. Chem.* **2014**, 754, 8.

[14] E. Güzel, S. Güney, M. Kandaz, *Dyes Pigm.* **2015**, 113, 416.

[15] E. Güzel, A. Koca, M. B. Koçak, *Supramol. Chem.* **2017**, 29, 536.

[16] İ. Gülçin, A. Z. Tel, A. C. Gören, P. Taslimi, S. H. Alwasel, *J. Food Meas. Charact.* **2019**, 13, 2062.

[17] H. Genç Bilgiçli, A. Kestane, P. Taslimi, O. Karabay, A. Bytyqi-Damoni, M. Zengin, İ. Gülçin, *Bioorg. Chem.* **2019**, 88, 102931.

[18] F. Turkan, A. Cetin, P. Taslimi, M. Karaman, İ. Gülçin, *Bioorg. Chem.* **2019**, 86, 420.

[19] K. Kucukoglu, H. I. Gul, P. Taslimi, I. Gulcin, C. T. Supuran, *Bioorg. Chem.* **2019**, 86, 316.

[20] B. Kuzu, M. Tan, P. Taslimi, İ. Gülçin, M. Taşpınar, N. Menges, *Bioorg. Chem.* **2019**, 86, 187.

[21] E. Güzel, N. Şaki, M. Akın, M. Nebioğlu, İ. Şişman, A. Erdoğmuş, M. B. Koçak, *Synth. Met.* **2018**, 245, 127.

[22] E. Güzel, *J. Turkish Chem. Soc. Sect. A Chem.* **2018**, 5, 1051.

[23] E. Bursal, A. Aras, Ö. Kılıç, P. Taslimi, A. C. Gören, İ. Gülçin, *J. Food Biochem.* **2019**, 43, e12776.

[24] U. Tutar, Ü. M. Koçyiğit, H. Gezegen, *J. Biochem. Mol. Toxicol.* **2019**, 33, e22281.

[25] İ. Timur, Ü. M. Kocyigit, T. Dastan, S. Sandal, A. O. Ceribası, P. Taslimi, İ. Gulcin, M. Koparir, M. Karatepe, M. Çiftçi, *J. Biochem. Mol. Toxicol.* **2019**, 33, e22239.

[26] U. M. Kocyigit, P. Taslimi, H. Gezegen, İ. Gülçin, M. Ceylan, *J. Biochem. Mol. Toxicol.* **2017**, 31, e21938.

[27] M. Huseynova, A. Medjidov, P. Taslimi, M. Aliyeva, *Bioorg. Chem.* **2019**, 83, 55.

[28] Y. Tao, Y. Zhang, Y. Cheng, Y. Wang, *Biomed. Chromatogr.* **2013**, 27, 148.

[29] M. T. Ibrahim, A. Uzairu, G. A. Shallangwa, S. Uba, *Scientific African* **2020**, 9, e00503.

[30] Y. Nicolet, O. Lockridge, P. Masson, J. C. Fontecilla-Camps, F. Nachon, *J. Biol. Chem.* **2003**, 278, 41141.

[31] X. Shen, W. Saburi, Z. Gai, K. Kato, T. Ojima-Kato, J. Yu, K. Komoda, Y. Kido, H. Matsui, H. Mori, M. Yao, *Acta Crystallogr., Sect. D: Biol. Crystallogr.* **2015**, *71*, 1382.

[32] F. J. Solis, R. J. B. Wets, *Math. Oper. Res.* **1981**, *6*, 19.

[33] G. Y. Atmaca, H. Yakan, H. Kutuk, M. Nebioğlu, E. Güzel, A. Erdogmuş, *J. Porphyr. Phthalocyanines* **2019**, *23*, 821.

[34] E. Güzel, M. N. Yarasir, A. R. Özkaya, *Synth. Met.* **2020**, *262*, 116331.

[35] X. Zheng, Y. Wang, J. Hu, G. Yang, Z. Guo, J. Xia, Z. Xu, G. Fang, *J. Mater. Chem. A* **2017**, *5*, 24416.

[36] E. Güzel, A. Koca, A. Gül, M. B. Koçak, *Synth. Met.* **2015**, *199*, 372.

[37] S. Kaya, S. Erkan, D. Karakaş, *Spectrochim. Acta, Part A* **2021**, *244*, 118829.

[38] A. Üngördü, K. Sayin, *Chem. Phys. Lett.* **2019**, *733*, 136677.

SUPPORTING INFORMATION

Additional Supporting Information may be found online in the supporting information tab for this article.